ELSEVIER

Journal of Non-Crystalline Solids 266–269 (2000) 1320–1324

JOURNAL OF NON-CRYSTALLINE SOLIDS

www.elsevier.com/locate/jnoncrysol

a-Si:H thin film transistors after very high strain

H. Gleskova [a,*], S. Wagner [a], Z. Suo [b]

[a] Department of Electrical Engineering, Princeton University, E-Quad., B-405, Olden St., Princeton, NJ 08544, USA
[b] Department of Mechanical and Aerospace Engineering and Princeton Materials Institute, Princeton University, Princeton, NJ 08544, USA

Abstract

We fabricate amorphous silicon (a-Si:H) thin-film transistors (TFTs) on a 25 μm Kapton foil, and then bend the foil over mandrels of various radii. The bending causes tensile strain in the TFTs when they face out, and compressive strain when they face in. After bending, we measure the electrical properties of the TFTs. After ∼2% of compressive strain, there is no change in the TFT electrical performance due to bending, namely in the on-current, off-current, source-gate leakage current, mobility and the threshold voltage. In tension, no change in the TFT performance is observed up to the strain of ∼0.5%. For larger tensile strains TFTs fail mechanically by cracking of the TFT layers. These cracks run perpendicularly to the bending direction.

1. Introduction

Much current research in thin film electronics is about on the fabrication of thin-film devices on plastic substrates [1–8] for applications that require non-breakable or flexible circuits.

In traditional thin film fabrication the substrate is stiff and much thicker than the deposited films. The films must conform to the substrate. While the substrate remains nearly stress-free, all stress is concentrated in the films. However, when the substrate is compliant, it becomes stressed, which reduces the stress in the film. We have analyzed theoretically this transition from stiff to compliant substrate materials [9]. Here we report measurements of the effects of bending on amorphous silicon (a-Si:H) thin-film transistors (TFTs) made on a 25 μm thick polyimide (Kapton E) foil.

2. Experimentals

All TFT silicon layers were deposited on 25 μm thick Kapton E foil at 150°C. The TFTs have the bottom gate, back-channel etch structure shown in Fig. 1. The channel length $L = 15$ μm and width $W = 210$ μm. The fabrication is described elsewhere [2].

The as-fabricated TFT/substrate structure had a built-in radius of curvature $R = 18$ mm, with the TFTs on the outside (stiff substrate, see Fig. 1(a)). On some devices we removed the stiff SiN_x layer from the back of the substrate (compliant substrate, see Fig. 1(b)). This reduced the radius of curvature of the structure to $R = 8$ mm, with the TFTs still on the outside.

Individual transistors were stressed mechanically by bending inward, as shown schematically in

* Corresponding author. Tel.: +1-609 258 3582; fax: +1-609 258 6279.
E-mail address: gleskova@ee.princeton.edu (H. Gleskova).

0022-3093/00/$ - see front matter
PII: S0022-3093(99)00944-8

Fig. 2, or outward. Single TFTs were bent to decreasing R, beginning with $R = 4$ mm down to $R = 0.5$ mm. The TFT was stressed for one minute at each bending radius, and then was released and remeasured.

We calculate the strain produced during the bending in the channel of the TFT. Assume that the substrate with thickness d_s and Young's modulus Y_s is covered on both sides with identical films, with Young's modulus Y_f and thicknesses d_{f1}

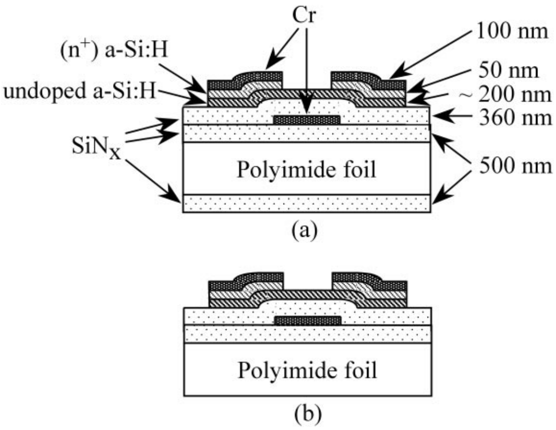

Fig. 1. Cross-section of a-Si:H TFT on 25 μm thick Kapton foil. (a) Stiff substrate – the as-fabricated sandwich structure; (b) compliant substrate – back SiN_x removed.

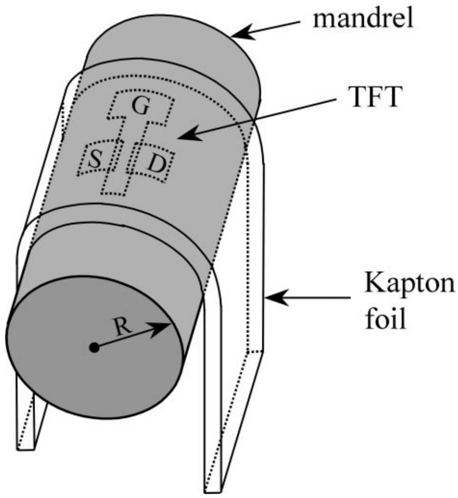

Fig. 2. Schematic of a TFT bent inward.

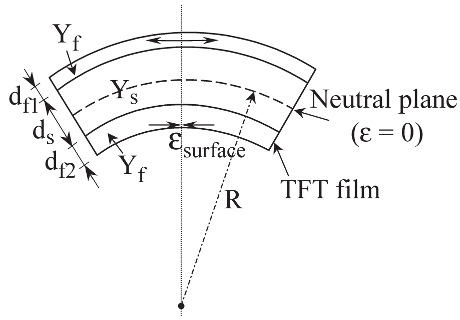

Fig. 3. Films-on-foil structure bent to a cylindrical roll.

and d_{f2}, as shown in Fig. 3. During the bending, the outside film is under tension while the inside film is under compression. The strain $\varepsilon_{surface}$ on the surface of the TFT sample bent to the radius of curvature R is [7]

$$\varepsilon_{surface} = \left(\frac{1}{R} \pm \frac{1}{R_0}\right)\frac{d_s + d_{f1} + d_{f2}}{2} \times \frac{\chi(\eta_1^2 + \eta_2^2) + 2(\chi\eta_1 + \chi\eta_1\eta_2 + \eta_2) + 1}{\chi(\eta_1 + \eta_2)^2 + (\eta_1 + \eta_2)(1 + \chi) + 1}, \tag{1}$$

where R_0 is the radius of curvature of the structure before applying the bending moment, $\chi = Y_f/Y_s$, $\eta_1 = d_{f1}/d_s$, and $\eta_2 = d_{f2}/d_s$. The plus (minus) sign denotes the case when the TFT sample before bending was on the opposite (same) side of the curvature than during the bending itself.

Table 1 summarizes the strain due to bending in the channel of TFTs, calculated using Eq. (1), for both structures of Fig. 1. In Table 1 one can see the effect of the back SiN_x layer on the amount of the strain in the TFT. Removing this layer reduces the strain in the TFT channel area by a factor of ~2.

3. Results

Fig. 4 summarizes the results of the inward (a, c) and outward (b, d) bending tests performed on TFTs fabricated on 25 μm thick Kapton foil. The top graphs show the on-current, I_{on}, the off-current, I_{off}, and the gate-leakage current, I_{leak}, as

Table 1
Bending strain in the channel area of the TFT calculated from Eq. (1)[a]

R (mm)	Inward bending		Outward bending	
	Strain (%) (without back SiN_x layer)	Strain (%) (with back SiN_x layer)	Strain (%) (without back SiN_x layer)	Strain (%) (with back SiN_x layer)
4	0.22	0.32	0.07	0.21
3	0.27	0.41	0.12	0.30
2.5	0.31	0.48 ± 0.01	0.16	0.37 ± 0.01
2	0.37 ± 0.01	0.59 ± 0.01	0.22 ± 0.01	0.47 ± 0.01
1.5	0.47 ± 0.01	0.77 ± 0.02	0.32 ± 0.01	0.65 ± 0.02
1	0.67 ± 0.03	1.12 ± 0.05	0.51 ± 0.03	1.00 ± 0.05
0.5	1.26 ± 0.12	2.18 ± 0.22	1.10 ± 0.12	2.07 ± 0.22

[a] $d_s = 25$ μm, $Y_s = 5$ GPa, $Y_f = 183$ GPa [11], $d_{f1} = 500$ nm and $d_{f2} = 960$ nm.

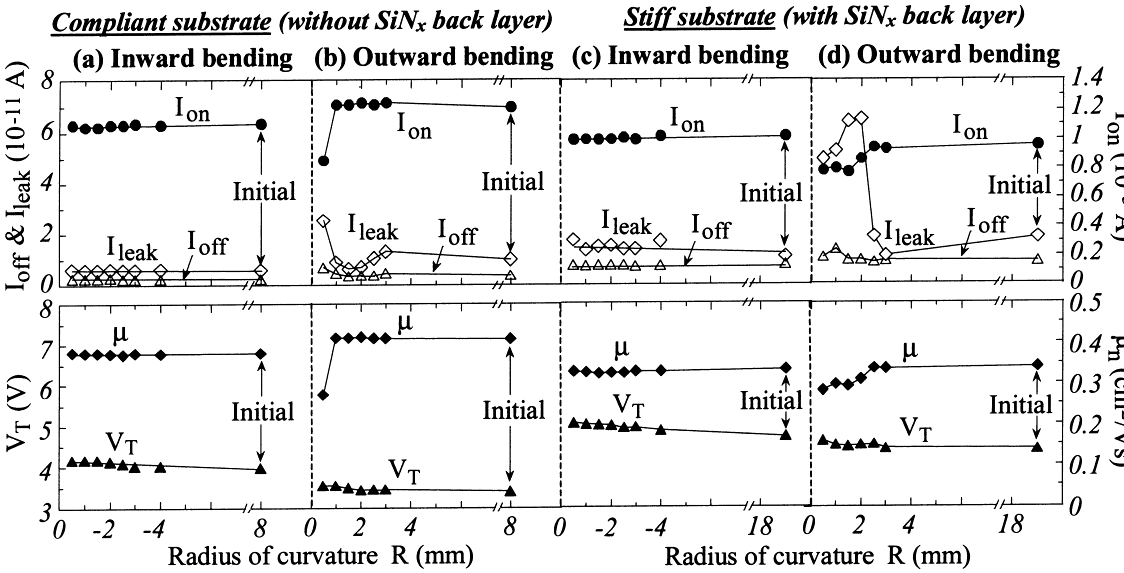

Fig. 4. On-(I_{on}), source-gate leakage (I_{leak}), off-currents (I_{off}), electron mobility μ_n and threshold voltage V_T in the saturation regime as functions of bending radius. I_{off} is the smallest source-drain current at $V_{ds} = 10$ V, I_{on} is the source-drain current for $V_{ds} = 10$ V and the gate voltage $V_{gs} = 20$ V and I_{leak} is the source-gate current for $V_{ds} = 10$ V and $V_{gs} = 20$ V. Outward bending R is defined positive, inward bending negative. Differences between the 'Initial' characteristics reflect spread between as-fabricated TFTs.

functions of the radius of curvature. The bottom graphs show the threshold voltage, V_T, and the saturated electron mobility, μ_n, calculated from the transfer characteristic at source-drain voltage $V_{ds} = 10$ V, as a function of the bending radius. For inward bending down to $R = 0.5$ mm, practically no change in I_{on}, I_{off}, I_{leak}, and μ_n, and only a continuous increase in V_T of less than 10% was observed, for both compliant and stiff substrates. At $R = 0.5$ mm the channel area of the TFTs was subjected to compressive strain of 2.18% for the stiff substrate, or 1.25% for the compliant substrate. The monotonic increase in the threshold voltage, observed in all cases, does not result from bending because a similar shift was observed in repeated measurements of unstressed TFTs.

During the outward bending, the samples are under tensile strain. In this configuration they fail mechanically at strain of ~0.5%. The samples on the stiff substrate fail at larger R than samples on

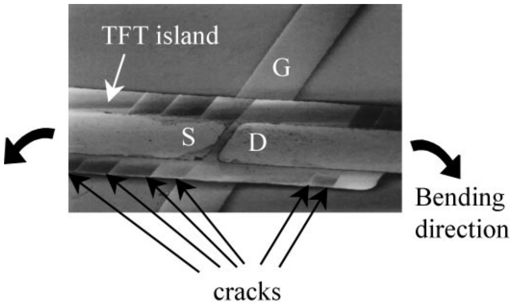

Fig. 5. SEM picture showing failure of a TFT with the SiN_x back layer (stiff substrate) bent outward. The TFT failed at $R = 2$ mm.

compliant substrate, as expected from the amount of calculated strain (see Table 1). For outward bending of the compliant substrate, there is no change in I_{on}, I_{off}, I_{leak}, μ_n and V_T down to $R = 1$ mm, which corresponds to a strain of $\leqslant 0.51\%$. For the outward bending of the stiff substrate, I_{on}, I_{off}, I_{leak}, μ_n and V_T do not change down to $R = 2.5$ mm which corresponds to a strain of $\leqslant 0.37\%$. For larger tensile strains some samples fail mechanically by cracking. An example of a samples with several cracks across TFT island is shown in Fig. 5. The cracks are perpendicular to the bending direction. Other samples function with deteriorated performance: I_{on} and μ_n decrease, I_{off} and I_{leak} increase. An example is shown in Fig. 4(d).

4. Discussion

a-Si:H TFT fabricated on steel [12] and Kapton have similar effects during outward bending. They function properly to a strain of ~0.5%. For larger strains the samples on steel delaminate, while about 50% of the samples on Kapton (stiff or compliant) still function with a deteriorated electrical performance. Inward bending produces different results for the samples on steel and Kapton foil. While the former delaminate at a strain of ~0.5%, the latter do not change their electrical performance up to a strain of ~2%. Mechanical failure during inward bending is triggered by delamination and depends on the size of a film/substrate debonded defect. Therefore, the smaller attainable strain in samples on steel may be caused by easier film delamination because of less adhesion between the steel substrate and the TFT structure than for Kapton substrates. Samples fabricated on Corning 7059 changed their electrical performance after being subjected to much smaller bending strain, but these devices cannot be compared directly to ours because they had Al source-drain contacts with no (n^+) a-Si:H layer [13].

5. Conclusions

Earlier experiments with bending TFTs on a 25-μm thick steel foil (a stiff substrate) have shown that a-Si:H TFTs can be strained by about 0.5% before failing mechanically at a radius of curvature R of ~2 mm [12]. Our present observation is that TFTs made on the same thickness of Kapton foil (either in a stiff or in a compliant configuration) function down to ~0.5% of tensile strain or ~2% of compressive strain without any change in their electrical performance.

Acknowledgements

We gratefully acknowledge support from the DARPA HDS program.

References

[1] G.N. Parsons, C.S. Yang, C.B. Arthur, T.M. Klein, L. Smith, Mater. Res. Soc. Symp. Proc. 508 (1998) 19.
[2] H. Gleskova, S. Wagner, Z. Suo, Mater. Res. Soc. Symp. Proc. 508 (1998) 73.
[3] J.N. Sandoe, Dig. Techn. Papers Soc. Information Display 29 (1998) 293.
[4] E. Lueder, M. Muecke, S. Polach, in: Proceedings of the International Display Research Conference, Asia Display '98, 1998, p. 173.
[5] A. Constant, S.G. Burns, H. Shanks, C. Gruber, A. Landin, D. Schmidt, C. Thielen, F. Olympie, T. Schumacher, J. Cobbs, Electrochemical Society Proceedings 94-35 (1995) 392.
[6] S.G. Burns, H. Shanks, A. Constant, C. Gruber, D. Schmidt, A. Landin, F. Olympie, The Electrochemical Society Proceedings 96-23 (1997) 382.

[7] S.D. Theiss, P.G. Carey, P.M. Smith, P. Wickboldt, T.W. Sigmon, Y.J. Tung, T.J. King, IEEE Int. Electron Devices Meeting 1998, Technical Digest, p. 257.
[8] D.B. Thomasson, M. Bonse, J.R. Huang, C.R. Wronski, T.N. Jackson, IEEE Int. Electron Devices Meeting 1998, Technical Digest, p. 253.
[9] Z. Suo, E.Y. Ma, H. Gleskova, S. Wagner, Appl. Phys. Lett. 74 (1999) 1177.
[10] H.Gleskova, S. Wagner, Z. Suo, Mater. Res. Soc. Symp. Proc. 557 (1999) 653.
[11] T.S. Hickernell, F.M. Fliegel, F.S. Hickernell, IEEE Ultrasonic Symposium Proceedings, vol. 1, IEEE, New York, 1990, p. 445.
[12] E.Y. Ma, S. Wagner, Mater. Res. Soc. Symp. Proc. 508 (1998) 13.
[13] B.L. Jones, J. Non-Cryst. Solids 77&78 (1985) 1405.